Available online at www.sciencedirect.com
ScienceDirect
Biochemical and Biophysical Research Communications 365 (2008) 1–7
BBRC
www.elsevier.com/locate/ybbrc

# Focal junctions retard lateral movement and disrupt fluid phase connectivity in the plasma membrane

Dina Vind-Kezunovic [a,*], Urszula Wojewodzka [b], Robert Gniadecki [a]

[a] Department of Dermatology, Bispebjerg Hospital, University of Copenhagen, Denmark
[b] Laboratory of Cell Ultrastructure, Polish Academy of Sciences, Warsaw, Poland

Received 4 October 2007
Available online 22 October 2007

**Abstract**

In cultured keratinocytes, focal junctions are enriched in major constituents of lipid rafts, such as $GM_1$ ganglioside, phosphoinositides, caveolins and flotillins. We have therefore speculated that focal junctions represent superrafts formed by coalescence of microdomains into large areas containing liquid-ordered ($L_o$) lipids. Indeed, values of maximal fluorescence recovery after photobleaching revealed that the long-range mobility of cholera toxin B subunit (CTB, marker of $L_o$) was ~1.5-fold retarded within the focal junctions compared to the surrounding membrane. However, 1,1′-dioctadecyl-3,3,3′,3′-tetramethylindocarbocyanine perchlorate (DiI-$C_{18:0}$), which specifically partitions to the liquid-disordered ($L_d$), non-raft phase, was also enriched in focal junctions and its mobility was slightly retarded. Cross-linking of $GM_1$ by CTB or raft aggregation by methyl-β-cyclodextrin further decreased the recovery of DiI-$C_{18:0}$. We propose a model in which focal junctions impose lateral heterogeneity in the plasma membrane by entrapment of lipid microdomains between dense arrays of immobilized transmembrane molecules which can enmesh otherwise freely percolating $L_d$ phase lipids.


*Keywords:* Focal junctions; Lipid rafts; Molecular mobility

The important property of plasma membranes in living cells is the approximately 5- to 50-fold retardation of lateral mobility in comparison to artificial lipid bilayers [1]. Limited lateral diffusion of the molecules creates membrane heterogeneity and compartmentalization of biochemical processes such as signal transduction and membrane sorting. There is evidence suggesting that arrays of transmembrane proteins subdivide the plasma membrane into submicron compartments of 30–230 nm. Molecular movement within a compartment occurs by brownian motion, whereas the migration between the compartments is retarded and occurs by hop-diffusion [1]. On a lower level, membrane proteins may bind and organize lipid molecules forming the so-called lipid shells of the size of approximately 7 nm [2]. The shells can further coalesce into larger units of lipid rafts (<200 nm) enriched in cholesterol, glycosphingolipids and sphingomyelin demonstrating the liquid-ordered ($L_o$) state contrasting with the more fluid liquid-disordered ($L_d$) portions of the membrane [3]. Assuming that different proteins and lipids partition specifically to $L_o$ or $L_d$ of the membrane, the presence of microdomains imposes constriction upon the percolation of the molecules [4]. Furthermore, the rafts may associate into larger functional entities sized 0.2–2 μm [5], the so-called superrafts, stabilized by lipid–protein interactions. It is however controversial whether formation of microdomains and liquid phase separation takes place in the membranes of living cells. Although clusters of $L_o$ domains can be produced by cross-linking of the raft component, $GM_1$ ganglioside by pentavalent cholera toxin B subunit (CTB), this phenomenon has been considered to have no physiological significance [6]. We have previously shown that CTB form patches in the human epidermis and in normal human keratinocytes [7]. In unattached HaCaT keratinocytes in suspension, CTB is homogeneously distributed in the

* Corresponding author. Fax: +45 35 31 60 10.
*E-mail address:* dv01@bbh.regionh.dk (D. Vind-Kezunovic).

0006-291X/$ - see front matter © 2007 Elsevier Inc. All rights reserved.
doi:10.1016/j.bbrc.2007.10.066

plasma membrane [8]. Upon attachment to coverslips CTB redistributes to the basal portion of the plasma membrane and coalesces into micrometer large patches [8]. We show here that $GM_1$ cross-linking is facilitated within focal junctions. Based on the co-clustering experiments and measurements of diffusional capacity by fluorescence recovery after photobleaching (FRAP) we propose that crowded, immobilized proteins within focal junctions may trap lipid microdomains leading to the formation of labyrinthine, sieve-like structures capable of retarding the lateral motion of non-raft proteins and lipids.

## Materials and methods

*Reagents.* Methyl-β-cyclodextrin, cholera toxin subunit B-conjugated fluorescein isothiocyanate (CTB-FITC) was purchased from Sigma–Aldrich (St. Louis, MO). 1,1′-Dioctadecyl-3,3,3′,3′-tetramethylindocarbocyanine perchlorate, cholera toxin subunit B Alexa Fluor 555 conjugate, Alexa Fluor 568 transferrin conjugate and Alexa Fluor 488 goat anti-mouse IgG were from Molecular Probes (Eugene, OR). Mouse anti-flotillin 1 and 2 and mouse anti-caveolin 1 and 2 antibodies were obtained from BD Biosciences (San Jose, CA). Integrin α4β1 P4G9 mouse anti-human antibody was from DAKO Corporation (Carpinteria, CA) and Texas Red conjugated goat anti-mouse antibody from Jackson ImmunoResearch Laboratories, Inc (West Grove, PA).

*Cell culture and treatment.* The spontaneously immortalized human keratinocyte cell line HaCaT [9] was a courtesy of Dr. M.R. Pittelkow, Mayo Clinic, Rochester, MN and cultured as previously described [10]. For FRAP experiments, cells were grown until subconfluence on four-well Lab-Tek chambered coverslips (Nunc, Roskilde, Denmark) or on 15 mm round coverslips. For cholesterol depletion, cells were washed twice in phosphate buffered saline (PBS) (Bie & Berntsen A-S, Herlev, Denmark), and incubated with 1–2% methyl-β-cyclodextrin (MβCD) dissolved in Dulbecco's modified Eagle's medium (DMEM) without phenol red (Gibco, Invitrogen, Taastrup, Denmark) as described [10]. In some experiments, quiescent or MβCD-treated cells were fixed with 4% paraformaldehyde (Bie & Berntsen) at 4 °C for 20 min or 4% glutardialdehyde dissolved in PBS for 16 h at 4 °C (KEBO Lab A/S, Albertslund, Denmark). For FRAP, fluorescein isothiocyanate tagged-CTB (CTB-FITC) was used at 2.5 μg/ml for 10 min at 4 °C. In experiments with double labelling, CTB-FITC was added together with secondary antibodies and diluted in PBS supplemented with 0.5% bovine serum albumin. Alexa Fluor 568 transferrin conjugate was used at a concentration of 50 μg/ml. For $L_d$ lipid staining, the cells were incubated with 1 μM DiI-$C_{18:0}$ (0.1% DMSO) for 30 min at 37 °C. Primary and secondary antibodies were diluted in 0.5% bovine serum albumin in PBS and used at 4 °C for 30 min.

*DNA constructs and transfection.* HaCaT cells were transiently transfected with PLCδ$_1$-PH-GFP wild-type and mutation constructs [11] using Lipofectamine™ LTX Reagent as described by the manufacturer (Invitrogen). The mutant R40L carries a mutation within the PH domain at position R40 (a critical basic residue), which abrogates the affinity to $PIP_2$ [11]. Twenty-four hours post-transfection, cells were washed in PBS, treated without or with 1% MβCD dissolved in DMEM without phenol red, washed and fixed with 2% paraformaldehyde for 10 min at room temperature (RT). After three washes in PBS, cells were stained with CTB-Alexa Fluor 555 for 30 min at RT.

*Confocal microscopy.* An Olympus IX70 inverted confocal microscope equipped with an argon–krypton laser and a 100× oil objective, NA 1.30 were used (Olympus, Fluoview). Excitation was provided by the 488 and 568 nm laser lines and emission was recorded at 510–540 or 585–640 nm, respectively. For FRAP, the pre-bleached image was recorded at 20% laser power. Then, a rectangular stripe of interest 1.2 μm-wide was irreversibly photobleached by repetitive scans at 100% laser power. Successive fluorescence recordings were obtained under the same conditions as the pre-bleached references at 30 s intervals for 870 s or until recovery completed at RT ~25 °C or at 37 °C using a Warner Culture Chamber Nr. 23 and a Single Channel Heater Controller, TC-324B (Warner Instruments, Hamden, CT). Fluorescence recovery was calculated as the percentage of fluorescence diffusing from the surrounding portions of the cell membrane to the bleached region compensated for the background bleaching as previously described [10]:

Fluorescence recovery (%) $= y_t u / x w_t$

where $u$ and $w_t$ are pre- and post-photobleaching fluorescence intensities outside the bleached region at time $t$, and $x$ and $y_t$ are, respectively, the pre- and post-bleach fluorescence intensities in the photobleached region at time $t$. The maximal fluorescence recovery ($B_{max}$) was extrapolated from one site hyperbola equation based on seven cells in each experimental condition to the experimental data obtained by the GraphPad Prism 3.03 package (GraphPad Software Inc, San Diego, CA). Statistical differences ($P < 0.05$, 12 degrees of freedom) in the approximated $B_{max}$ values for fluorescence recovery were estimated by the unpaired $t$-test.

## Results

### *Focal junctions are enriched in lipid raft constituents*

We have previously described that in living keratinocytes in suspension, staining with fluorescently tagged CTB reveals a homogeneous staining of the membrane even after prolonged incubations with this compound [8]. Upon attachment to coverslips CTB redistributes to the basal portion of plasma membrane and coalesces into micrometer large patches [8], which are enriched in cholesterol [12] and resemble junctional structures. We have therefore investigated whether CTB co-localizes with integrins of focal junctions and with selected lipid raft markers. Double staining with CTB-FITC and antibody directed against focal junction-related α4β1 integrin demonstrated co-localization of both markers. Also perfect overlaps between CTB and caveolin 1 and 2 or flotillin 1 and 2 were observed (Fig. 1). As integrins are attached to the substratum and therefore not movable, these data indicated that raft cross-linking by CTB is facilitated within adhesional structures in unpertubed cells.

More lines of evidence supported this notion. Phosphoinositol 4,5-bisphosphate ($PIP_2$) is concentrated in lipid rafts [13]. We demonstrated that the wild-type pleckstrin homology (PH) domain of phospholipase C (PLC)δ$_1$ tagged to a green fluorescent protein [11], which is a non-cross-linking probe that binds to $PIP_2$, co-localizes strongly with CTB within $CTB^{bright}$ patches (Fig. 2A–C) in contrast to the R40L inactive mutant construct (Fig. 2D–F). Moreover, $CTB^{bright}$ patches were found in cells pre-fixed with glutaraldehyde for >16 h (Fig. 2G) or after fixation with 4% paraformaldehyde (data not shown).

### *Focal junctions are also enriched in $L_d$ phase markers*

It is widely accepted that CTB-$GM_1$ complexes partition to $L_o$ domains, making CTB the preferred marker of $L_o$ and raft environment [14–16]. Therefore we hypothesized that the $CTB^{bright}$ patches within focal junctions represent superrafts in $L_o$ phase. If true, one could predict that these

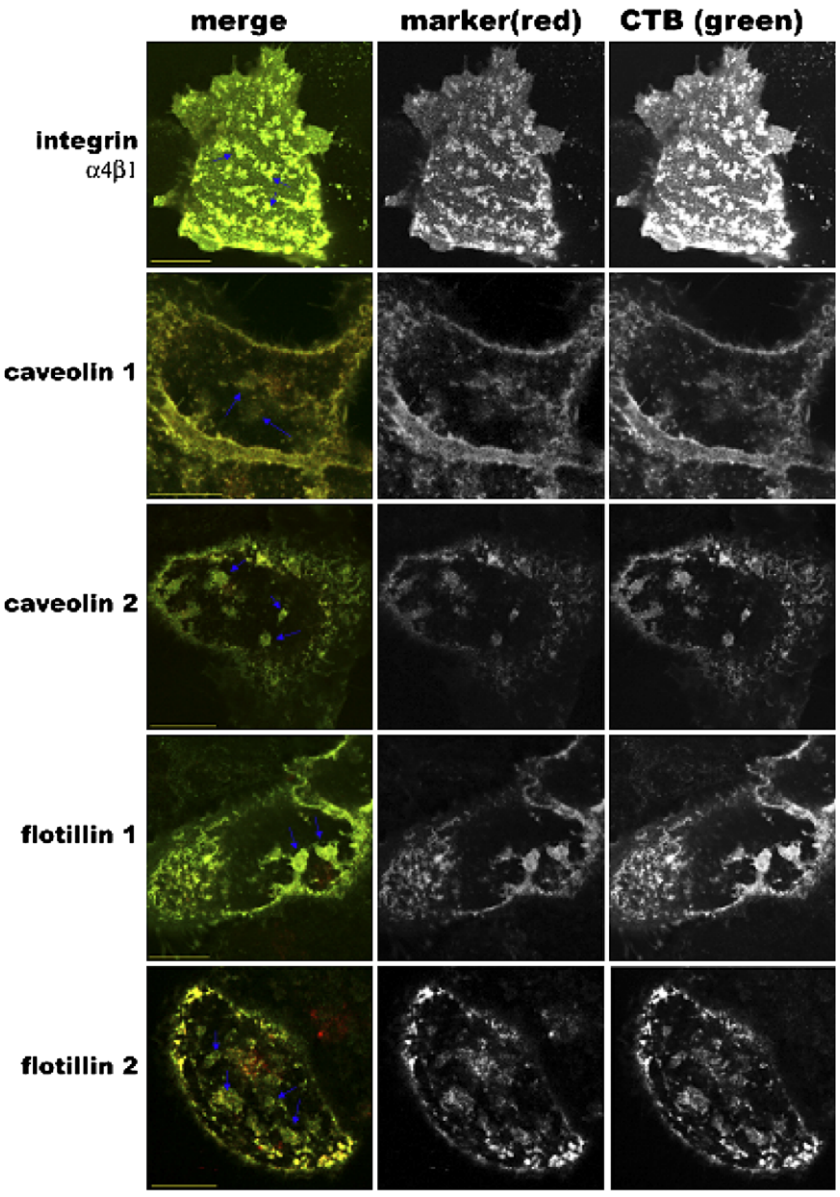


Fig. 1. Co-localization of α4β1 integrin with lipid raft markers. $GM_1$ ganglioside in subconfluent HaCaT cells was clustered with pentavalent CTB-FITC and the cells were stained with antibodies directed against focal junction-related integrin α4β1 and selected lipid raft markers: caveolin 1 and 2, flotillin 1 and 2 for 30 min at 4 °C followed by Texas Red-conjugated secondary antibodies. Blue arrows: focal junctions. Scale bar, 10 μm.

structures would be depleted of $L_d$ phase lipids. We tested this prediction by labelling the $L_d$ phase by lipid probe 1,1′-dioctadecyl-3,3,3′,3′-tetramethylindocarbocyanine perchlorate (DiI-$C_{18:0}$) [16,17] and by visualizing the distribution of the transferrin receptor, the partitioning of which is not affected by the $L_o/L_d$ state of membrane lipids [18]. Unexpectedly, DiI-$C_{18:0}$ overlapped perfectly with α4β1 integrin within $CTB^{bright}$ regions (Fig. 3D–F). Within $CTB^{bright}$ domains, we also observed an increased staining by both DiI-$C_{18:0}$ (Fig. 3A–C) and the Alexa Fluor 568 conjugated transferrin (TfR-AF), respectively (Fig. 3G–I). DiI-$C_{18:0}$ staining did not represent a secondary redistribution of the dye due to $GM_1$ cross-linking with CTB as seen in giant unilamellar vesicles [14,15], since DiI-$C_{18:0}{}^{bright}$ patches depicted by arrows (Fig 3J) were seen in intact, living cells stained solely with this dye. Subsequently added CTB co-localized with the DiI-$C_{18:0}{}^{bright}$ structures (Fig. 3L–O). This finding further indicated that CTB patches do not occur at random but reflects pre-existing structures in the membranes, most probably focal junctions.

### *Restriction of lateral mobility within focal junctions*

One of the possible hypotheses emerging from the above-presented data is that focal junctions are not mere superrafts but rather labyrinthine, meshwork-like $L_o$-enriched structures that may entrap proteins and lipids percolating in the $L_d$ phase through the plasma membrane.

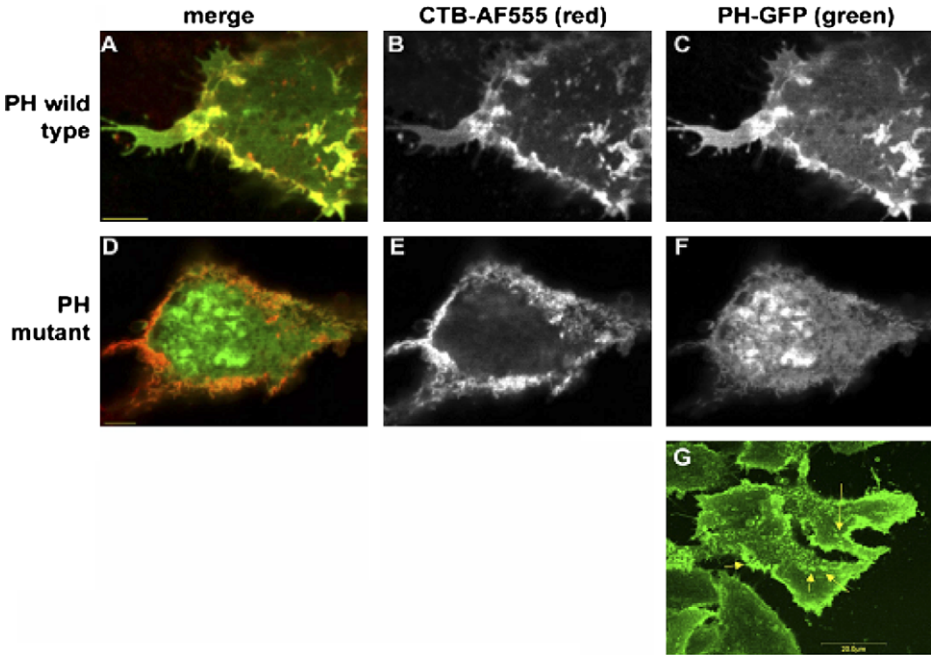


Fig. 2. Co-localization of wild-type PLC$\delta_1$-PH-GFP and $GM_1$ ganglioside clustered with CTB-AF555. Subconfluent HaCaT keratinocytes were transfected with wild-type $PIP_2$-sequestering PH domain of the phospholipase C$\delta_1$-fused to green fluorescent protein, wild-type PLC$\delta_1$-PH-GFP (A–C) or the mutant R40L, which does not bind $PIP_2$ (D–F). Twenty-four hours post-transfection cells were fixed in paraformaldehyde and stained with Alexa Fluor 555 conjugated-CTB for 30 min at RT. (A,D) Overlap images of red (B,E) and green (C,F) fluorescence channels. Note the overlap of $GM_1$-CTB and the wild-type PH-GFP in (A), but segregation of $GM_1$-CTB and the PH-GFP mutant in (D). Scale bar, 10 μm. (G) $CTB^{bright}$ patches are found in glutaraldehyde fixed cells. Subconfluent HaCaT cells were fixed for 16 h at 4 °C with 4% glutaraldehyde. After wash, the cells were stained with CTB-FITC for 1 h at RT before confocal microscopy imaging. Focal junctions stained with CTB-FITC are marked with arrows. Scale bar, 20 μm.

To test this hypothesis we directly measured the long-range diffusional mobility of different molecules by FRAP. According to the rationale developed by Simons and co-workers [4] the value of maximal recovery after photobleaching would be decreased below 100% both at room temperature ~25 °C and at 37 °C if molecular motion and the ability to percolate through the membrane is restricted. As shown in Fig. 4A, the $L_d$ marker, DiI-$C_{18:0}$ showed as expected an almost complete recovery (89.1% ± 8.3% [SEM], NS versus 100%) in the DiI-$C_{18:0}^{dim}$ regions of the basal portion of the membrane. These data indicated a free percolation of the dye in the range of micrometers. Maximal recovery (80.0% ± 6.8% [SEM]) was slightly lower within the DiI-$C_{18:0}^{bright}$ focal junctions (Fig. 4A) but the difference did not reach statistical significance. However, when $GM_1$ ganglioside was cross-linked by CTB, DiI-$C_{18:0}$ displayed a 18.0% and 19.6% decrease in fluorescence recovery in $CTB^{dim}$ and focal junction-$CTB^{bright}$ areas, respectively (Fig. 4B). The efficacy of $GM_1$ cross-linking was higher within focal junctions and was reflected by a more pronounced decrease in CTB fluorescence recovery to the level of 44.5% ± 3.6% [SEM] versus 70.1% ± 4.8% [SEM] in the bulk membrane ($P < 0.05$, $t$-test) (Fig. 4B). CTB displayed the same recovery pattern in double-labelling experiments with TfR-AF (Fig. 4C). The recovery of TfR was also lower within the $CTB^{bright}$ patches compared to the non-raft compartment. A rise of the temperature from 25 to 37 °C did not lead to a complete recovery of CTB or TfR neither within $CTB^{bright}$ domains nor in the surrounding membrane (Fig. 4D). This indicated that the partial recovery was caused by a membrane compartmentalization rather than global decrease of molecular diffusion.

Extraction of cholesterol from the membrane by MβCD [19] disrupts the normal structure of cholesterol-dependent microdomains, such as lipid rafts. After treatment with MβCD, the patchy staining on the bottom membrane was still present but the main part of the membrane was poorly stained and the $GM_1$ was distributed homogenously at the periphery at the cell. MβCD-treatment did not impede the molecular mobility of DiI-$C_{18:0}$ when CTB-FITC staining was omitted (Fig. 4A). When double staining with CTB-FITC and DiI-$C_{18:0}$ was performed, MβCD-treatment caused a significant decrease in the recovery of DiI-$C_{18:0}$ (Fig. 4E) by 31% within the junctions and by 46% in the basal membrane outside the focal junctions ($P < 0.05$, $t$-test). Moreover, MβCD-treatment caused a significantly decreased recovery of $L_o$-associated CTB to 38.8% ± 2.8% [SEM] within the focal junctions and 56.0% ± 4.8% [SEM] in the surrounding membrane (Fig. 4E). Also, a 2% 30 min MβCD-treatment restricted the molecular mobility of CTB and TfR at RT with 23% and 34%, respectively, within $CTB^{bright}$ domains and 30% and 31%, respectively, within the $CTB^{dim}$ bulk membrane ($P < 0.05$, $t$-test) (Fig. 4F). A rise from 25 to 37 °C did not lead to an increase in fluorescence recovery in MβCD-treated cells except for a slight increase of TfR within $CTB^{bright}$ domains (36.0% ± 3.8 [SEM] versus

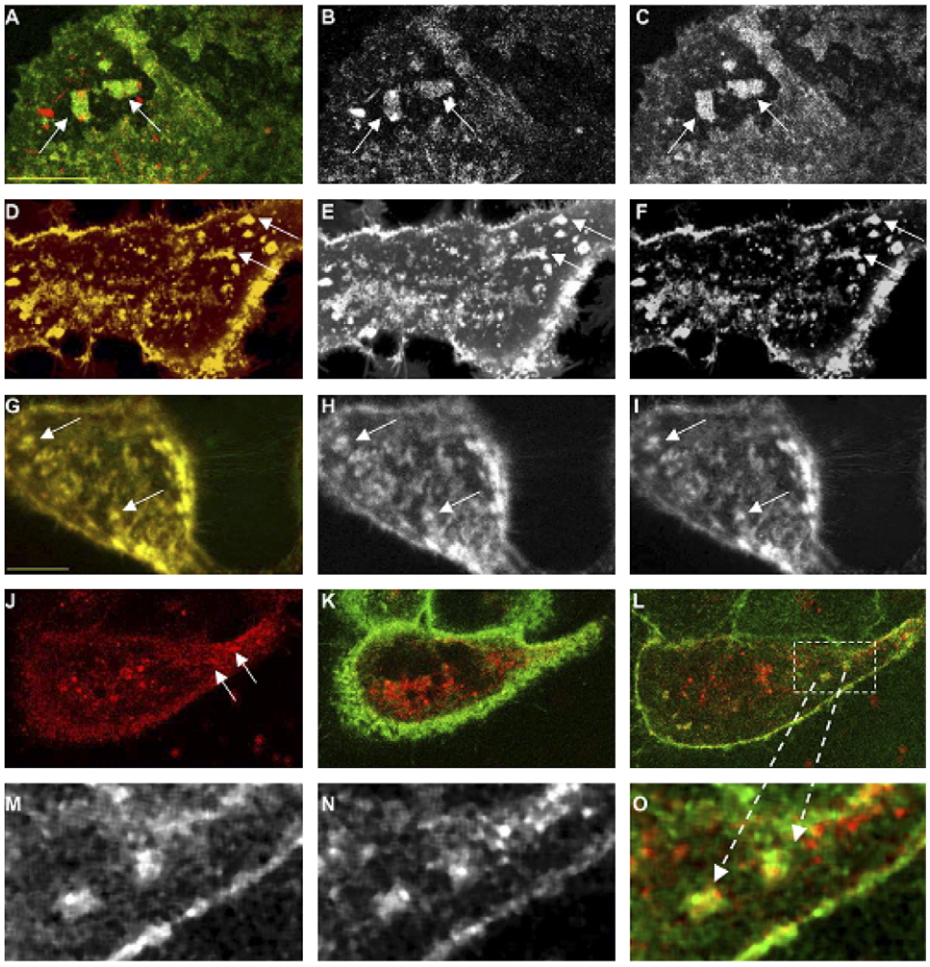


Fig. 3. Accumulation of $L_d$ markers in focal junctions. (A–F) Cells were stained with DiI-$C_{18:0}$ (30 min, 37 °C) (red fluorescence) and labelled with CTB-FITC (green fluorescence) for 10 min at 4 °C (A–C) or fixed in paraformaldehyde followed by labelling against α4β1 integrin (green fluorescence) (D–F). (G–I) Simultaneous staining with CTB-FITC and Alexa Fluor 568 conjugated-transferrin for 10 min at 4 °C. (A,D,G) Overlap images of red (B,E,H) and green (C,F,I) fluorescence channels. (J–O) Cells were stained with DiI-$C_{18:0}$ as described in methods and imaged by confocal microscopy (J) followed by labelling with CTB-FITC for 15 min at RT while resting in the same position on the microscope, and imaged instantly (K) and after 30 min (L,O). Short arrows in (A–J): focal junctions showing co-localization of the markers. Focal junctions labelled by DiI-$C_{18:0}$ and CTB-FITC (white dashed arrows) are magnified in (O) showing overlap of green CTB fluorescence (M) and red DiI-$C_{18:0}$ fluorescence (N). Scale bars: 10 μm.

49.2% ± 4.6 [SEM]; $P < 0.05$, $t$-test) (Fig. 4G). Taken together, our data indicate that $L_o$ domain cross-linking can decrease percolation of the $L_d$ phase via physical entrapment of the molecules between dense islands of $L_o$ lipids. The effect of MβCD is similar to that of domain cross-linking with CTB and is likely to reflect coalescence of lipid rafts into larger units enmeshing $L_d$ lipids and causing a decrease in their percolation (Fig. 4H and I).

## Discussion

Recent research has shown that in biological membranes the lipids exist in the immiscible fluid–fluid phases. The $L_o$ phase is organized hierarchically into different classes of microdomains, ranging from lipid shells (<10 nm in diameter), lipid rafts (<200 nm diameter) to the superrafts (size range of micrometers) [3]. However, the mechanisms, which govern $L_o/L_d$ regulation and phase separation, remain unknown. One recognized factor causing large-scale phase separation in biological membranes is cross-linking of the $L_o$ lipids, such as $GM_1$ ganglioside by pentavalent CTB [14].

Our data support the two-phase fluid model of biological membranes, as recently proposed by the group of Simons [4]. On the basis of FRAP studies of the apical membrane of polarized epithelial cells, they proposed the co-existence of $L_o$ and $L_d$ phases in which one is discontinuous and the other fully percolating (connected, as defined by the fluorescence recovery at infinity in FRAP experiment). Our data also show that in the bulk membrane, the $L_d$ phase is fully percolating in contrast to CTB-$GM_1$. The new finding here is that focal junctions define the regions where the connectivity of both $L_o$ and $L_d$ phases is deceased. This finding is in line with recent data showing the $L_o$ lipid order and the presence of caveolin in focal junctions in endothelial cells [20].

An unexpected finding was an apparent juxtaposition of $L_d$ and $L_o$ regions within the focal junctions, especially evi-

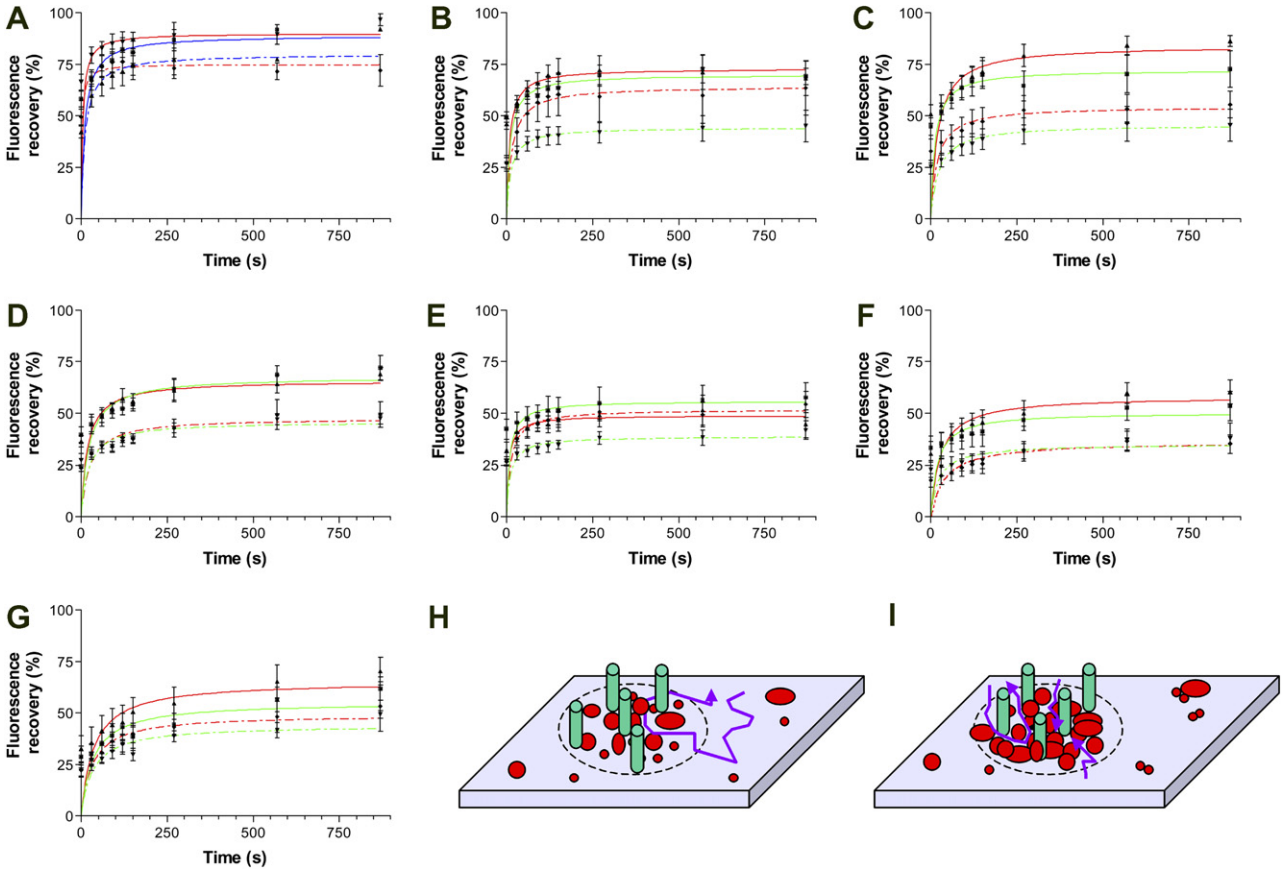


Fig. 4. FRAP analysis of molecular mobility within focal junctions. FRAP was performed as described in methods at RT ~25 °C (A–C,E,F) or at 37 °C (D,G) using a thermostatic Warner Culture Chamber. Graphs show the theoretically fitted curves of fluorescence recovery in % and the error bars represent standard errors of the mean (SEM). (A) Cells stained with DiI-$C_{18:0}$ alone (30 min, 37 °C) (blue curves; controls) or were subsequently incubated with 1% MβCD for 15 min at 37 °C (red curves). *Dashed curves;* DiI-$C_{18:0}^{bright}$ focal junctions; *solid curves*; DiI-$C_{18:0}^{dim}$ bulk membrane. (B–G) *Dashed curves*: $CTB^{bright}$ focal junctions; *solid curves*; $CTB^{dim}$ bulk membrane. (B) Cells were stained with DiI-$C_{18:0}$ as described in (A) and subsequently labelled with CTB-FITC for 10 min at 4 °C. *Red*: DiI-$C_{18:0}$; *green*: CTB-FITC. (C,D) Cells were incubated simultaneously with CTB-FITC and Alexa Fluor 568-conjugated human transferrin (10 min, 4 °C) at RT (C) or at 37 °C (D). *Red*: TfR-AF; *green*: CTB-FITC. (E) Cells were stained with DiI-$C_{18:0}$ as described in (A) and treated with 1% MβCD (15 min, 37 °C) before CTB-FITC staining. *Red*: DiI-$C_{18:0}$; *green*: CTB-FITC. (F,G) Subconfluent HaCaT cells were treated with 2% MβCD (30 min, 37 °C) and FRAP was performed at RT (F) or at 37 °C (G). *Red*: TfR-AF; *green*: CTB-FITC. (H,I) A model of membrane dynamics within focal junctions. (H) Focal junctions contain high concentrations of lipid raft-like domains (*red ovals*), probably via their entrapment by arrays of transmembrane proteins (*green cylinders*). These domains form meshwork-like structures that retard the motion (*purple arrow*) of $L_d$ phase (*blue*). (I) These effects are emphasized by $L_o$ domain cross-linking by CTB or their coalescence in cholesterol-depleted cells in which the $L_d$ phase becomes enmeshed within the dense labyrinth of $L_o$ domains resulting in a loss of phase connectivity.

dent from the FRAP experiments showing that connectivity of $L_d$ phase is dramatically decreased by domain cross-linking or coalescence, either by CTB-$GM_1$ complexing or by cholesterol extraction by MβCD. Thus, focal junctions cannot be viewed as superraft-like structures in a way, which has been proposed for the enterocyte brush border [21], the immunological synapse [22], or the leading edge of migrating cells [23]. Our data are rather compatible with the recent model of membrane organization proposed by the group of Davis [24]. By electron microscopy they showed the existence of protein- and cholesterol-poor areas of the membrane (probably enriched in $L_d$ fluid phase) and the protein-rich islands. The latter could be further subdivided into raft-enriched and raft-poor regions.

We propose that focal junctions are a specialized variant of such protein-enriched regions containing both $L_o$, raft-like domains enriched in $GM_1$ ganglioside, flotillins, caveolins and phosphoinositides, and non-raft regions labelled by DiI-$C_{18:0}$. It is likely that $L_o$ lipid domains create a labyrinthine array, which entraps non-raft components and $L_d$ lipids, thus limiting their percolation. Such an array is probably created by enmeshment of $L_o$ domains between the immobilized transmembrane proteins within the junctions. It is known that transmembrane proteins affect motion of the lipids by a simple mechanic impediment of diffusion [1] or due to lipid–protein interaction leading to the formation of lipid shells [2]. Protein density within focal junctions is believed to be high with the expected distance of 5–100 nm between single molecules [25]. It is in the size range of lipid shell and lipid raft domains. It is thus likely that movement of rafts through the junctions is delayed due to collisions with the immobilized transmembrane proteins.

Fluid–fluid phase separation is functionally important since it directly alters the lateral distribution and function

of membrane proteins [15]. One of the implications of our finding is a testable hypothesis that focal junctions are particularly sensitive to alterations in lipid phase mixing and provide sensors for extracellular cross-linking events. Domain cross-linking could provide biologically relevant stimuli able to precipitate signal transduction from the focal junctions.

## Acknowledgments

We thank M. Edidin (The John Hopkins University, Baltimore, MD) for providing the PLC$\delta_1$-PH-GFP plasmids with permission of T. Balla (Endocrinology and Reproduction Research Branch, NIH, Bethesda, MD). We thank E. Hoffmann and I. Pedersen for preparation of cell cultures and G. Larsen, Bio-Science, Gilleleje, Denmark for technical assistance. Aage Bang Foundation and Jeppe Juhl and wife Ovita Juhl Foundation financially supported this work.

## References

[1] A. Kusumi, H. Ike, C. Nakada, K. Murase, T. Fujiwara, Single-molecule tracking of membrane molecules: plasma membrane compartmentalization and dynamic assembly of raft-philic signaling molecules, Semin. Immunol. 17 (2005) 3–21.

[2] R.G. Anderson, K. Jacobson, A role for lipid shells in targeting proteins to caveolae, rafts, and other lipid domains, Science 296 (2002) 1821–1825.

[3] L.J. Pike, Rafts defined: a report on the keystone symposium on lipid rafts and cell function, J. Lipid Res. 47 (2006) 1597–1598.

[4] D. Meder, M.J. Moreno, P. Verkade, W.L. Vaz, K. Simons, Phase coexistence and connectivity in the apical membrane of polarized epithelial cells, Proc. Natl. Acad. Sci. USA 103 (2006) 329–334.

[5] G.J. Schutz, G. Kada, V.P. Pastushenko, H. Schindler, Properties of lipid microdomains in a muscle cell membrane visualized by single molecule microscopy, EMBO J. 19 (2000) 892–901.

[6] E.A. Merritt, S. Sarfaty, F. Van den Akker, C. L'Hoir, J.A. Martial, W.G. Hol, Crystal structure of cholera toxin B-pentamer bound to receptor GM1 pentasaccharide, Protein Sci. 3 (1994) 166–175.

[7] R. Gniadecki, B. Bang, Flotillas of lipid rafts in transit amplifying cell-like keratinocytes, J. Invest. Dermatol. 121 (2003) 522–528.

[8] R. Gniadecki, N. Christoffersen, H.C. Wulf, Cholesterol-rich plasma membrane domains (lipid rafts) in keratinocytes: importance in the baseline and UVA-induced generation of reactive oxygen species, J. Invest. Dermatol. 118 (2002) 582–588.

[9] P. Boukamp, R.T. Petrussevska, D. Breitkreutz, J. Hornung, A. Markham, N.E. Fusenig, Normal keratinization in a spontaneously immortalized aneuploid human keratinocyte cell line, J. Cell Biol. 106 (1988) 761–771.

[10] S. Lambert, D. Vind-Kezunovic, S. Karvinen, R. Gniadecki, Ligand-independent activation of the EGFR by lipid raft disruption, J. Invest. Dermatol. 126 (2006) 954–962.

[11] P. Varnai, T. Balla, Visualization of phosphoinositides that bind pleckstrin homology domains: calcium- and agonist-induced dynamic changes and relationship to myo-[3*H*] inositol-labeled phosphoinositide pools, J. Cell Biol. 143 (1998) 501–510.

[12] B. Bang, R. Gniadecki, B. Gajkowska, Disruption of lipid rafts causes apoptotic cell death in HaCaT keratinocytes, Exp. Dermatol. 14 (2005) 266–272.

[13] L.J. Pike, J.M. Miller, Cholesterol depletion delocalizes phosphatidylinositol bisphosphate and inhibits hormone-stimulated phosphatidylinositol turnover, J. Biol. Chem. 273 (1998) 22298–22304.

[14] K. Bacia, P. Schwille, T. Kurzchalia, Sterol structure determines the separation of phases and the curvature of the liquid-ordered phase in model membranes, Proc. Natl. Acad. Sci. USA 102 (2005) 3272–3277.

[15] A.T. Hammond, F.A. Heberle, T. Baumgart, D. Holowka, B. Baird, G.W. Feigenson, Crosslinking a lipid raft component triggers liquid ordered-liquid disordered phase separation in model plasma membranes, Proc. Natl. Acad. Sci. USA 102 (2005) 6320–6325.

[16] N. Kahya, D. Scherfeld, K. Bacia, B. Poolman, P. Schwille, Probing lipid mobility of raft-exhibiting model membranes by fluorescence correlation spectroscopy, J. Biol. Chem. 278 (2003) 28109–28115.

[17] K. Bacia, D. Scherfeld, N. Kahya, P. Schwille, Fluorescence correlation spectroscopy relates rafts in model and native membranes, Biophys. J. 87 (2004) 1034–1043.

[18] T. Harder, P. Scheiffele, P. Verkade, K. Simons, Lipid domain structure of the plasma membrane revealed by patching of membrane components, J. Cell Biol. 141 (1998) 929–942.

[19] Y. Ohtani, T. Irie, K. Uekama, K. Fukunaga, J. Pitha, Differential effects of alpha-, beta- and gamma-cyclodextrins on human erythrocytes, Eur. J. Biochem. 186 (1989) 17–22.

[20] K. Gaus, S. Le Lay, N. Balasubramanian, M.A. Schwartz, Integrin-mediated adhesion regulates membrane order, J. Cell Biol. 174 (2006) 725–734.

[21] E.M. Danielsen, G.H. Hansen, Lipid raft organization and function in brush borders of epithelial cells, Mol. Membr. Biol. 23 (2006) 71–79.

[22] A. Viola, S. Schroeder, Y. Sakakibara, A.T. Lanzavecchia, T lymphocyte costimulation mediated by reorganization of membrane microdomains, Science 283 (1999) 680–682.

[23] C. Gomez-Mouton, J.L. Abad, E. Mira, R.A. Lacalle, E. Gallardo, S. Jimenez-Baranda, I. Illa, A. Bernad, S. Manes, C. Martinez-A, Segregation of leading-edge and uropod components into specific lipid rafts during T cell polarization, Proc. Natl. Acad. Sci. USA 98 (2001) 9642–9647.

[24] B.F. Lillemeier, J.R. Pfeiffer, Z. Surviladze, B.S. Wilson, M.M. Davis, Plasma membrane-associated proteins are clustered into islands attached to the cytoskeleton, Proc. Natl. Acad. Sci. USA 103 (2006) 18992–18997.

[25] K. Jacobson, O.G. Mouritsen, R.G. Anderson, Lipid rafts: at a crossroad between cell biology and physics, Nat. Cell Biol. 9 (2007) 7–14.